Metabolomics Vol. 1, No. 1, January 2005 (© 2005)
DOI: 10.1007/s11306-005-1108-2

Comprehensive two-dimensional gas chromatography–time-of-flight mass spectrometry (GC × GC-TOF) for high resolution metabolomics: biomarker discovery on spleen tissue extracts of obese NZO compared to lean C57BL/6 mice

Werner Welthagen,[a,b] Robert A. Shellie,[c] Joachim Spranger,[d,e] Michael Ristow,[d,e] Ralf Zimmermann,[a,b,f] and Oliver Fiehn[g]

[a]*Institute of Ecological Chemistry, GSF-Research Centre, Oberschleißheim, D-85764, Germany*
[b]*Analytical Chemistry, University of Augsburg, Augsburg, D-86159, Germany*
[c]*Max-Planck-Institute of Molecular Plant Physiology, 14424, Potsdam, Germany*
[d]*German Institute of Human Nutrition, Potsdam-Rehbrücke, Germany*
[e]*Charité University Medicine Berlin, Germany*
[f]*BIfA – Bavarian Institute of Applied Environmental Research and Technology, Augsburg, D-86167, Germany*
[g]*Genome Center, University of California, Davis, CA, 95616-8816, USA*

Received 25 August 2004; accepted 1 September 2004

Comprehensive two-dimensional gas chromatography–time-of-flight mass spectrometry (GC × GC-TOF) was applied for the analysis of complex metabolite profiles from mouse spleen. The resulting two-dimensional chromatograms proved that mass spectral quality and sensitivity were largely improved by the enhanced resolution and zone compression, which are features of GC × GC operation, when compared to classical one-dimensional GC-TOF methods. The improved peak capacity of GC × GC allowed for peaks to be detected that could previously not be separated in one-dimensional GC. A measure of the combined power of chromatographic and mass spectral deconvolution resolution is called "analytical purity", with higher values indicating less pure peaks. GC × GC-TOF lead to the detection of 1200 compounds with purity better than 0.2, compared to 500 compounds with purity up to 2.5 in one-dimensional GC-TOF. The compounds identified include many of the compounds previously reported in NMR studies and other methods on mammalian tissues. Spleen samples of several obese NZO mice and lean C57BL/6 control strains were analyzed in order to demonstrate the applicability of GC × GC-TOF for biomarker identification.

KEY WORDS: Obesity, metabonomics; metabolic profiling; type 2 diabetes mellitus; nutrigenomics.

Introduction

A comprehensive and individual characterization of all the metabolites present in a given biological situation (metabolomics) is a challenging task for instrumental analysis. In the past 5 years, metabolomic strategies (Fiehn, 2002) have been developed mainly in the field of plant biology, with various applications being published (Weckwerth, 2004). These applications range from unraveling plant gene functions in physiological contexts (Weckwerth *et al.*, 2004a), to unbiased detection of unexpected metabolic responses under environmental stress conditions (Hirai *et al.*, 2004) or co-regulation of biochemical pathways that are commonly mapped far apart from each other (Fiehn, 2003). Protocols are adapted, tested and validated also for other organisms like bacteria (Wittmann *et al.*, 2004). Furthermore, alternative strategies have been applied to characterize global metabolic fingerprints in mammalian samples mainly by nuclear magnetic resonance spectroscopy (NMR) (Nicholson *et al.*, 1996). NMR metabolic fingerprinting offers the advantage of truly quantitative measurements compared to mass spectrometry (MS), which relies on calibration or relative quantitations. However, NMR analyses lack the resolution and sensitivity required to individually quantify and identify the whole suite of metabolites present in typical biological samples. Typically, less than 30 signals can be referred to specific metabolites in NMR metabolic fingerprints (Keun *et al.*, 2002; Wang *et al.*, 2003).

The chemical diversity of metabolites can better be covered if at least two different physicochemical properties are exploited, like in gas chromatography–mass spectrometry (GC–MS: volatility and mass) (Fiehn *et al.*, 2000a, b) or high performance liquid chromatography–mass spectrometry (LC–MS: hydrophobicity and mass) (Tolstikov *et al.*, 2003). The combination of data from GC–MS and monolithic-LC–MS runs with the application of appropriate data deconvolution and extraction techniques enables the detection of some 1400 individual (and genuine) metabolites. The overlap between LC–MS and GC–MS with respect to the range of detectable compounds is limited due to the differences in

*To whom correspondence should be addressed.
E-mail: ofiehn@ucdavis.edu

separation and ionization mechanisms. An alternative global approach that applied three different methods based on capillary electrophoresis (CE) coupled to mass spectrometry was elaborated, in which more than 1600 metabolites from *B. subtilis* cultures were detected (Sato *et al.*, 2002). Although CE/MS is definitely stronger than GC–MS, NMR or LC–MS with respect to phosphorylated or sulfated small molecules, it seems to be less suitable for secondary metabolites and lipophilic compounds. Difficulties with scaling up injection volumes and capillary diameters further render CE/MS a less suitable choice with respect to elucidating unknown structures by fractionation and subsequent MS^n and NMR analysis.

Researchers have recently tried to utilize the high resolution of electrospray-ion cyclotron resonance-FT/MS for annotating individual changes in metabolome composition (Hirai *et al.*, 2004). Although direct infusion-MS may be easily applied for sample classification (Vaidyanathan *et al.*, 2001; Allen *et al.*, 2003; Scholz *et al.*, 2004), relative quantitation of individual metabolites is problematic, due to severe physical limitations such as ion suppression (Schmidt *et al.*, 2003) and adduct formation. These fundamental constraints are hardly solvable by current instrumentation, and lead to major analytical errors in the comparison of samples from different matrices, or in situations where largely altered metabolite abundances occur, such as in comparisons of plant mutants or stress conditions.

A combination of GC–MS and LC–MS may be regarded as benchmark technique; however, with respect to metabolome coverage, further improvements are needed. Here we demonstrate for the first time in metabolomic analysis the use of a technique which significantly enhances metabolite resolution: comprehensive two-dimensional gas chromatography/time-of-flight mass spectrometry (GC × GC-TOF). For proof of concept we have selected an application in mammalian biology: a comparison of two well-characterized mice strains, namely obese NZO mice and C57BL/6 control strains; and we exemplify how such profiles can be used for biomarker detection. Spleen tissue was selected as target for two reasons: (a) no report on metabolic profiles or NMR-based metabolic fingerprints from spleen extracts has been published so far, and (b) obesity and overfeeding have been demonstrated to negatively affect immune response in humans as well as rodents (Lamas *et al.*, 2004). We propose that metabolomics might help in elucidating the underlying mechanisms.

Experimental

Mice were housed in standard barrier facilities according to Federation of European Laboratory Animal Science Associations (FELASA) regulations and were fed standard chow (Altromin GmbH, Lage, Germany). Spleen tissues were garnered from five female, non-fasted, 10 months old lean C57BL/6 control strain and four female, non-fasted, 10 months old obese NZO strain mice. Five milligram fresh weight samples were extracted at −15 °C with 1 ml of a mixture of degassed H_2O:MeOH:$CHCl_3$ (2:5:2, v/v/v) and shaken for 5 min at 4 °C (Weckwerth *et al.*, 2004b). An aliquot of 500 μL was concentrated to complete dryness. The dry residue was dissolved in 20 μL of methoxamine hydrochloride (40 mg/ml pyridine) and incubated at 30 °C for 90 min with continuous shaking. Then 80 μL of *N*-methyl-*N*-trimethylsilyltrifluoroacetamide (MSTFA) was added to exchange acidic protons at 37 °C for 30 min. The derivatized samples were stored at room temperature for 120 min before injection. A GC × GC system (Agilent GC 6890, Agilent Technologies, USA; OPTIC III injector ATAS, The Netherlands; cryogenic modulator and secondary oven: LECO Inc., USA) was coupled to a time-of-flight mass spectrometer (Pegasus III, Leco Inc., USA). The 4-jet cryogenic modulator uses two liquid nitrogen cooled jets and two hot gas jets for efficient trapping and re-desorption (gating) of the analytes (Ledford and Billesbach, 2000; Kristenson *et al.*, 2003). Data acquisition and analysis was performed with a special software package (ChromaTOF software, Version 2.00, LECO Inc., USA). A two-column GC × GC column set was used for all analyses, made up of a 30 m × 250 μm (0.25 μm film thickness) dimethyl polysiloxane (Rtx-1MS, Restek Corp., USA) first-dimension column, coupled to a 1.5 m × 100 μm (0.10 μm film thickness) 50% phenyl polysilphenylene-siloxane (BPX-50, SGE, Australia) second dimension column (press fit connection). Each column was installed in an individual, independently temperature programmable GC oven. The primary GC oven (which housed the first-dimension column) was temperature programmed from 50 °C (held for 8 min) to 310 °C at 5 °C/min. The secondary oven (second dimension column) was temperature programmed from 56 °C (held for 10 min) to 300 °C at 5 °C/min. A modulation period of 3.0 s was used. Constant flow rate was used calculated from a linear flow rate of 20 cm/s at 25 °C. All injections (1 μL) were performed in split mode (1:2) at a constant injector temperature of 250 °C. The MS transfer line temperature was kept at 280 °C, the ion-source temperature was held constant at 250 °C, and the detector voltage was −1.8 kV. Data were acquired at 100 spectra/s (40–400 m/z). One-dimensional GC-TOF separation was performed on a 30 m × 250 μm (0.25 μm film) dimethyl polysiloxane (Rtx-1MS Restek) column under otherwise same conditions as the two-dimensional separations except a 10-fold higher sample injection due to lower sensitivity in GC-TOF compared to GC × GC-TOF.

Results and discussion

Chromatograms of mouse spleen extracts (polar fraction) exhibit a medium complexity when compared

to other specimen such as plant leaf samples. In figure 1, one- and two-dimensional separations of a spleen extract are compared as total ion current (TIC) based chromatograms. In one-dimensional GC-TOF chromatograms (Figure 1a), 538 peaks were detected after deconvolution and artifact removal. There were many amino- and hydroxy acids among these detected peaks, but a limited number of (plant typical) carbohydrate derivatives were observed (supplemental table S1). Compared to early results from plant metabolite profiling by GC-quadrupole MS and manual chromatogram inspection (Fiehn *et al.*, 2000a, b), the use of GC-TOF and mass spectral deconvolution increases the number of detectable peaks by a factor of three (Weckwerth *et al.*, 2004a). Mass spectral deconvolution is based upon slight differences in the time evolution of ions belonging specifically to different near co-eluting compounds. Not all of the detected peaks are immediately visible in the TIC chromatogram because a high proportion of them are present as minor and/or poorly resolved components. The apparent difference between the number of detectable peaks and the number of visibly plotted peaks in TIC chromatograms (peak heights in figure 1a) highlights the importance of the data treatment by mass spectral deconvolution. The majority of low abundance peaks can only be observed by plotting a series of unique ion chromatograms, using the unique ions that the software automatically finds and reports for each detected peak. Despite these improvements, the deconvolution approach fails for fully co-eluting peaks or near co-elution of minor species with intense main compounds. This is specifically problematic when multiple chromatograms are to be compared: in such cases, subtle chromatographic shifts will cause overlapping of previously separated peaks, causing false negative peak detections and hence missing values.

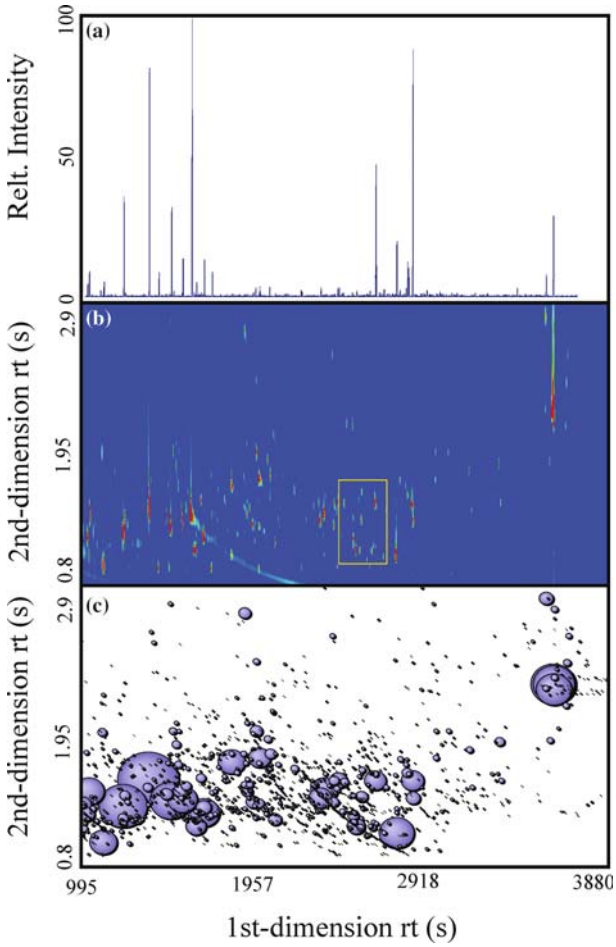

Figure 1. A comparison of a GC-TOF chromatogram analyzed independently (1a, top panel) with a GC × GC-TOF two-dimensional chromatogram (1b, middle panel) of a NZO female mouse spleen extract. The lower panel (1c) is a bubble plot representation of the identified peaks in the GC × GC chromatogram after the removal of known artifacts, with the bubble radius indicating the TIC intensity.

GC × GC-TOF enhances resolution and thus reduces the problem of co-eluting peaks (Marriott, 2002). Comprehensive two-dimensional gas chromatography (GC × GC) was developed in the early 1990s (Liu and Philipps, 1991, Phillips and Xu, 1995), and uses two serially coupled GC columns to separate compounds according to two different chromatographic selectivity parameters. The cryogenic modulation interface between the two columns traps the eluted analytes from the first column for a short time and then releases them into the second column (Phillips and Beens, 1999; Marriott and Kinghorn, 2000). Following the conventions of the majority of published GC × GC applications (Marriott and Shellie, 2002), we have chosen to perform first-dimension separation on a relatively non-polar column, in which the separation approximates a boiling point separation, while the second separation was performed on a fast isothermal (moderately polar) 50%-phenyl coated column for compound class separation based on the components' relative polarity. As the second chromatographic separation lasts only some seconds (we here used a modulation period of 3 s), and since peak widths in GC × GC are as narrow as 20 ms, a very fast responding detector is required. With spectral acquisition rates of up to 500 s^{-1} a time-of-flight mass spectrometer is ideally suited for fast-GC (van Deursen *et al.*, 2000) and thus also for GC × GC, specifically for separation of complex mixtures (Dallüge *et al.*, 2002a; Dallüge *et al.*, 2002b). The total run time from GC-TOF analysis of 65 min was pulsed into 1000 individual 3s modulation slices for GC × GC-TOF with an acquisition rate of 100 spectra/s, resulting in a total file size of 700 MB. Peak detection and deconvolution of GC × GC-TOF chromatograms was performed as described above and was complemented by combination of thermally modulated peaks using the vendor's ChromaTOF software. With a personal computer of 768 MB RAM and 2.0 GHz speed raw data processing took less than 30 min per sample.

Surprisingly, even for medium-complex samples like mouse spleen polar extracts, GC × GC-TOF revealed a

considerably higher number of separated peaks (Figure 1b, peak intensity is given in color code from light blue to red). In excess of 1220 peaks were counted following data treatment by deconvolution and removal of known artifacts such as polysiloxanes, phthalates or column bleed. Figure panel 1c gives a bubble plot representation of the same GC × GC-TOF chromatogram as in figure 1b, in which the size of the bubbles represents the TIC area of the respective chromatographic peaks. In comparison to figure 1b, this type of bubble plot presentation allows an improved overview of the peak distribution in the two-dimensional plane (Welthagen *et al.*, 2003; Shellie *et al.*, 2003). Table 1 gives a comparison of GC-TOF to GC × GC-TOF with respect to the resulting number and mass spectral quality of peaks. It becomes clear that overall, not only was the number of detectable metabolic peaks again increased by more than 2-fold, but also that analytical purity was greatly improved. Analytical purity refers to the combination of chromatographic resolving power and mass spectra deconvolution power. Therefore a compound may co-elute with other compounds yet still be pure if it's spectrum contains unique features relative to the co-eluting compounds. Obviously, it is more likely to achieve good purity if the chromatographic resolution is enhanced as in the case of GC × GC-TOF. Purity approaches zero in the optimal case and can theoretically reach infinitum in problematic cases. We have found that spectra with purity < 1.0 are often the most trustworthy. Specifically for high throughput and unsupervised operation it is highly mandatory that only large and pure peaks are compiled in the list of target compounds. It is a clear advantage of GC × GC-TOF analysis that there are about 7-fold more abundant and high quality peaks compared to one-dimensional GC-TOF, as defined by the threshold combination of S/N > 50 and purity < 1. This finding was observed despite the total number of high abundance peaks being comparable and despite the roughly 10-fold lower sample injection into GC × GC-TOF. This enhanced mass spectral quality is also reflected by the comparison of mean and median purity: most peaks in GC × GC-TOF match the required quality thresholds. Correspondingly, such peaks are more easily identifiable by matching to external spectral libraries and result in higher reliability in comparative quantifications between chromatograms.

Table 1
Comparison of number and quality of peaks by GC × GC-TOF and GC-TOF from a mouse spleen extract after removal of known measurement artifacts

	GC-TOF	GC × GC-TOF
# Compounds	538	1227
# With S/N > 50, Purity < 1	79	563
# With S/N > 100	202	342
Median purity	1.9	0.2
Mean purity	2.2	0.4
Median S/N	63	47
Mean S/N	411	310

Note: Threshold for peak detection was a signal/noise (S/N) ratio > 10.

A more detailed investigation of figure 1 leads to further insights to the advantages of GC × GC applications. For example, some problems with injection of silylated compounds are more clearly highlighted in GC × GC than with one-dimensional GC–MS: thermolabile compounds may partially decompose in the hot injector leading to characteristic sickle shaped extended peak tailing (Beens *et al.*, 1998). An example of this is seen for tris-trimethylsilyated phosphoric acid (which partially also stems from decomposition of organic phosphates), visibly tailing in figure 1b from about 1500–2100 s. This peak tail was therefore regarded as artifact and removed from the data set (as seen in figure 1c) applying classification rules based on its mass spectrum. It should be noted that this unusual peak shape is not a result of GC × GC, it is simply more noticeable in GC × GC than in one-dimensional GC, where the low intensity peak tail would disappear below the chemical baseline (Shellie *et al.*, 2002). Despite the number of detectable peaks, only 126 peaks were positively identified based on first-dimension retention index and mass spectral similarity when compared to a user library of 500 reference compounds (Figure 2 and supplemental table S1). Apart from classical biomedical targets such as glucose, fatty acids, amino acids and cholesterol, a range of other compounds were identified, among them dicarboxylic acids, aromatics and phosphorylated sugars.

In figure 1b, a small area is marked (box) which is analyzed and discussed in more detail in the following

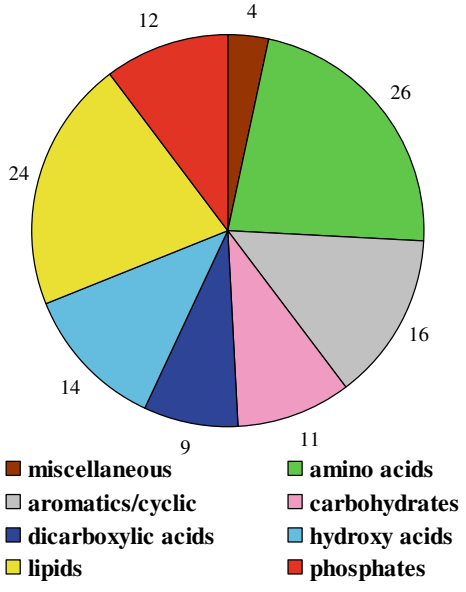

Figure 2. Compilation of identified peaks in GC-TOF based on first-dimension retention index and mass spectral similarity (see supplemental information table S1).

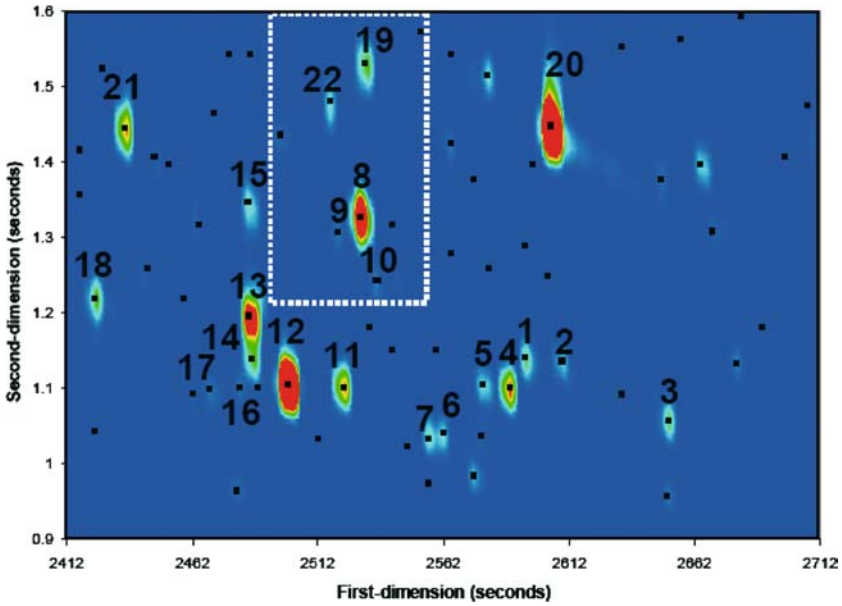

Figure 3. An extracted section from figure 1, showing the number of peaks detected (peak markers, black dots). Exemplary characterization of compounds is listed in table 2 (see supplemental information S2).

section. An enlarged representation of this area is shown in figure 3. The peak apex of each deconvoluted chromatographic peak is represented by the peak markers (black dots). In total 69 separated peaks are found in this small section, from which 22 of the more abundant components are labeled by numbers and annotated in table 2. Furthermore their deconvoluted mass spectra are available as supplementary material S2. Most mass spectra show the characteristics of sugar alcohols such as inositol-like species, based on mass spectral similarity and retention indices of allo-inositol or methylinositol (ononitol). For a further identification, however, authentic references compounds are needed. Nevertheless, the sheer complexity of detected sugar alcohol analogues might add potential hypotheses to the well-known involvement of inositol-phosphates in signaling cascades, which have been associated with diseases like diabetes and cancer (Cantley, 2002; Pendaries *et al.*, 2003) both known to be caused and/or promoted by elevated body weight (Adami and Trichopoulos, 2003). Within the section marked by the indicated box in figure 3, two peaks (#8 and #19) are present which completely co-elute in the first-dimension and thus can be taken as an example to demonstrate the enhancement of resolving power gained by the GC × GC approach. One of the two peaks (#8) is identified as ascorbate with a unique ion signal at 332 m/z, while the second peak (#19) indicates an unclassified and low abundant compound with a unique ion trace at 260 m/z. In figure 4 the corresponding section of the one-dimensional GC-TOF chromatogram is shown at the selected ion traces of 260 and 332 m/z (left panel). Complete co-elution of these two compounds hampers the spectral quality of the more abundant compound (#8, ascorbate) and renders the minor compound (#19) undetectable (false negative). In comparison, these two compounds can be nicely separated by GC × GC-TOF (figure 4, right panel) with baseline separation in the second chromatographic dimension. This serves as an example of why (a) considerably more compounds are detected in GC × GC-TOF than in one-dimensional GC-TOF, and equally important, why (b) the mean spectral purity in two-dimensional analysis was largely improved. One could argue that these peaks would have been separable in a one-dimensional GC-TOF run using a column of different polarity. However, although this is certainly true for a specific peak pair, this would only be achievable at the price of creating new co-elutions among the 1200 detectable compounds. With a lack of a universally applicable procedure for stationary phase selection, one may initiate a process of trial-and-error in the hope of identifying a specific stationary phase column that produces a globally optimized separation. However this still might not resolve key biomarker compounds. Conversely, GC × GC has the capacity to resolve many more peaks in a single one-shot analysis than any one-dimensional GC separation (of equivalent time). The three main benefits of the GC × GC-TOF approach are therefore (1) the maximum comprehensive separation obtainable within a single chromatographic run, (2) the increased average mass spectral purities and (3) the increased sensitivity obtained by the zone compression property of the cryogenic modulation (Lee *et al.*, 2001). This is specifically important in studies that go beyond manual interpretation of chromatograms, but focus at high-throughput and high-quality routine operation in metabolomics, specifically with respect to an enhanced quality of database entries in automated sample identi-

Table 2
Statistical comparison of the NZO and C57BL/6 samples based on the normalized TIC areas of the peaks #1–22 (see figure 2)

Characterization	#1 Sugar alcohol	#2 Sugar alcohol	#3 Alloinositol	#4 Sugar alcohol	#5 Sugar alcohol	#6 Sugar alcohol	#7 Sugar alcohol	#8 Ascorbate	#9 Hexa-decanol	#10 Aliphate	#11 Glucose 2
#1 C57BL/6	56,720	52,250	92,612	73,081	42,061	63,604	72,299	120,720	14,332	24,352	327,211
#2 C57BL/6	62,135	58,085	65,086	66,772	44,549	49,052	54,050	184,949	17,229	43,653	95,061
#3 C57BL/6	71,009	58,267	68,591	169,460	65,843	41,146	60,940	449,600	29,179	46,648	167,862
#4 C57BL/6	78,088	88,013	52,562	102,396	58,584	112,483	9851	358,179	45,786	42,319	77,751
#5 C57BL/6	56,944	48,898	76,960	99,842	30,035	109,734	16,133	285,096	19,837	14,967	203,468
#6 NZO	96,930	78,118	73,496	492,382	82,530	22,620	35,512	377,627	12,209	23,472	514,798
#7 NZO	30,731	48,500	58,140	176,200	28,115	16,238	27,539	217,621	3225	22,039	201,053
#8 NZO	28,149	18,394	60,806	144,819	30,190	9784	17,337	235,705	360,274	14,068	105,187
#9 NZO	67,572	58,657	69,998	319,683	57,940	47,486	7110	595,831	25,265	48,833	195,967
t-Test	0.31	0.25	0.25	0.05	0.46	0.01	0.09	0.25	0.23	0.24	0.23
	#12 Glucose 1	#13 1-Methyl-glucoside	#14 Hexose per-TMS	#15 Carbohydrate	#16 Fructose 1	#17 Fructose 2	#18 Carbohydrate	#19 Unknown	#20 Palmitic acid	#21 Dehydro-ascorbate	#22 Unknown
#1 C57BL/6	1,708,058	401,629	62,354	27,735	65,472	51,881	60,959	128,229	1,285,134	249,157	70,254
#2 C57BL/6	561,250	410,345	45,363	67,510	24,839	30,289	59,338	108,346	1,371,230	170,164	62,444
#3 C57BL/6	974,027	372,706	117,987	87,977	7626	28,465	111,313	138,522	1,418,236	200,697	51,634
#4 C57BL/6	453,153	260,279	61,865	61,209	70,256	81,543	82,691	143,997	1,581,389	134,817	59,684
#5 C57BL/6	1,148,108	378,136	61,777	75,590	27,198	32,014	1,11,015	168,731	1,483,671	286,296	98,586
#6 NZO	2,396,508	3,21,972	279,864	49,650	61,950	36,373	129,275	91,555	1,374,199	1,374,199	36,545
#7 NZO	1,123,571	200,498	114,618	50,604	55,310	27,644	81,006	48205	1,710,279	84,244	53,513
#8 NZO	627,186	176,794	78,270	27,066	27,188	14,926	61,855	58,689	10,102,294	90,059	29,556
#9 NZO	1,215,808	342,825	187,833	63,270	35,696	31,863	79,870	78,558	1,452,628	1,47,252	37,160
t-Test	0.22	0.04	0.06	0.12	0.35	0.09	0.44	0.001	0.19	0.27	0.01

Note: Peaks are characterized by likely compound class based on mass spectral features if identity is unclear. Methoximated sugars result in double peaks (as for glucose and fructose) with incomplete derivatization resulting in peak #14.

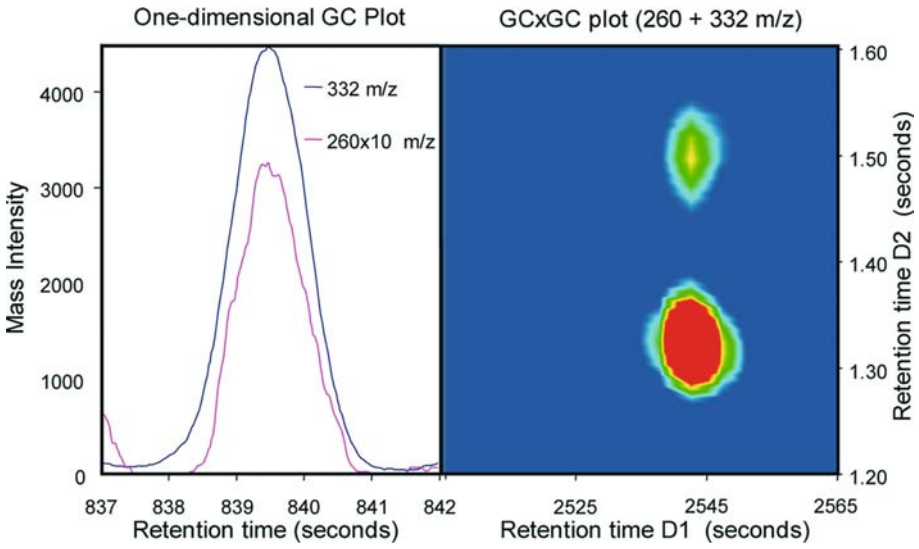

Figure 4. The co-elution of two peaks is indistinguishable in 1D GC-TOF (left panel), but clearly separated in GC × GC-TOF (right panel). The more abundant peak is identified as ascorbate with a unique ion signal at 332 m/z, whereas and the unknown compound has a unique ion of 260 m/z. The intensity of ion m/z 260 is given with a 10-fold enlargement in the one-dimensional GC-TOF ion chromatogram.

fication routines. Apart from an in-depth method validation for high-throughput operation with respect to ruggedness, accuracy and reproducibility of quantitation, it is foreseeable that long-term data storage and handling may get problematic with respect to the large size of the raw data files.

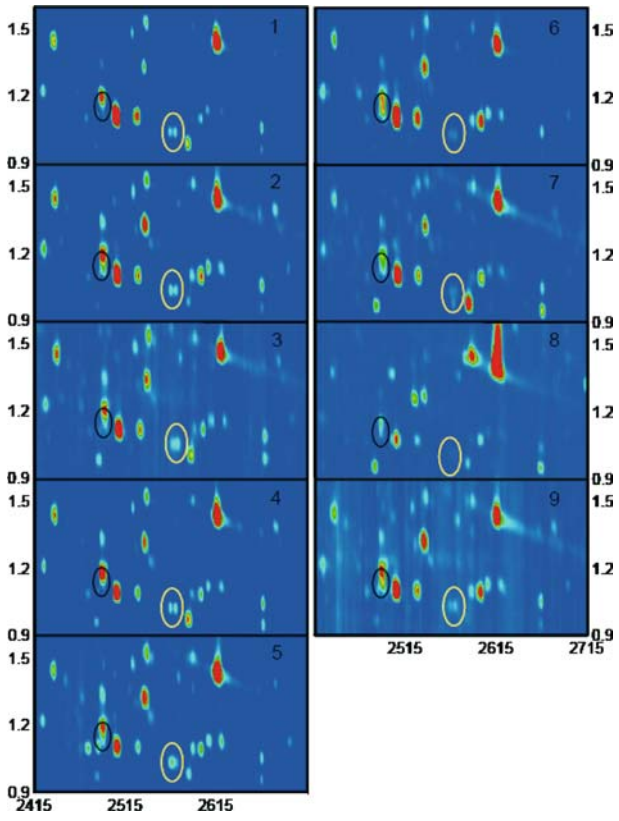

Figure 5. A direct comparison between the analyzed C57BL/6 female mouse spleen samples (left panel, samples 1–5) with the NZO female mouse samples (right panel, samples 6–9). The encircled compounds were used for exemplary statistical evaluation (table 2) of biomarker efficiency.

To demonstrate the usefulness of GC × GC-TOF for differential metabolomic biomarker identifications, four non-fasted female NZO obese mice (#6–9) were compared to five non-fasted female C57BL/6 controls (#1–5). Sections of the corresponding nine GC × GC-chromatograms are depicted in figure 5 using the same retention selection as indicated in figure 1. On the one hand, the chromatograms demonstrate the method reproducibility (i.e. stability of the separation pattern). For larger series of runs, potential shifts in first-dimension retention times can easily be corrected for by using retention index markers. For shifts in the second dimension, absolute peak shifts are regularly less than the total peak widths which therefore gives an estimate for peak finding windows in differential analyses of series of chromatograms. On the other hand, in figure 5 the biological variability between the individual mice becomes visually clear by the relative intensity differences among the metabolites of either the control strain samples (left panel) or the NZO mice spleen extracts (right panel). Such biological variability largely exceeds the analytical error measured by repeated injections of identical extracts (~5–10% relative standard deviation). Although the individuals belong to isogenic lines held under controlled environmental conditions, such a biological variability is the expected result of metabolic snapshots (Steuer *et al.*, 2003). Still, systematic differences can be observed which could be considered as potential obesity biomarkers: apparently, two sugar alcohols (peaks #6 and #7, indicated by yellow circles, numbering according to figure 3) are relatively less abundant in NZO spleen tissues compared to C57BL/6 samples. To demonstrate a way to find differences be-

tween the two mice groups (NZO and C57BL/6), the peak areas of the individual peaks labeled in figure 3 were normalized to the total area of all detectable peaks (after removing artifacts). Then, data were compared by Student's *t*-test (although it should be noted that the number of biological replicates *n* was too small to achieve actual statistical significance levels). Results are given in table 2 indicating that sugar alcohol #6 might indeed be different between the two groups whereas peak #7 had to be manually integrated to match the significance thresholds since it was below S/N > 20 in some of the obese NZO samples. Black circles in figure 5 indicate 1-methylglycoside (peak #13) from figure 3: applying a *t*-test on the normalized peak areas, 1-methylglycoside is also found as potentially different between the two mouse populations which was not visually apparent from the TIC chromatograms, as well as a further sugar alcohol (peak #4). Such initial hypotheses might then be tested by examining larger populations in order to gain statistical significance. Interestingly, the highest significance level and therefore the most likely obesity biomarker was found for peak #19: this was an unclassified, low abundant compound that was not separable from ascorbate in one-dimensional GC-TOF but only detectable by GC × GC-TOF. It is interesting to note that the most prominent metabolic changes in obese mice spleens were not related to classical analytical targets such as free fatty acids, glucose or cholesterol but to sugar alcohols and unidentified compounds. This finding indicates the prospects as well as the problems of this technique for biomarker discovery: the technique is mature and can directly be applied for biomedical research; however, the diversity of the metabolome and the difficulties in *de novo* identifications of GC–MS peaks (Fiehn *et al*., 2000b) disable a direct and easy route to mapping differences in biochemical pathways.

Conclusion

It was demonstrated that extending GC–MS to the level of comprehensive GC × GC-TOF analysis is directly applicable to differential metabolomic analysis of mammalian tissues. Apart from the increased number of safely detectable peaks, the most important feature is the enhanced spectral purity, which improves mass spectral deconvolution and similarity matches. This will certainly improve the data quality in biomedical data bases, if this technique is employed in larger research projects. In a proof-of-concept study on spleen extracts from lean versus obese mice strains, it was shown that data extraction and normalization tools are ready to be used for tentative biomarker detection. However, biological variability demands a sufficient number of biological replicates to be analyzed in order to suffice the required statistical power.

Acknowledgments

This work was financed through the GSF-research center, the Max-Planck-Society and the German ministry of education and research (BMBF), BioProfile Nutrigenomics Berlin/Brandenburg, BMBF project number 0313036B/C. We thank Änne Eckardt for quality control of extraction and GC-TOF standard operation procedures. Werner Welthagen thanks the Bayerische Forschungsstiftung (BFS) for a scholarship. Michael Ristow is funded by the Deutsche Forschungsgemeinschaft and Fritz-Thyssen-Stiftung. Dr. R. Kluge and Dr. H.G. Joost gratefully provided NZO mice, and Dr. C. Thöne-Reinecke helped with animal handling.

References

Adami, H.O. and Trichopoulos, D. (2003). Obesity and mortality from cancer. *N. Engl. J. Med.* **348**, 1623–1624.

Allen, J., Davey, H.M. and Broadhurst, D. (2003). High throughput classification of yeast mutants for functional genomics using metabolic footprinting. *Nat. Biotechnol.*. **21**, 692–696.

Beens, J., Tijssen, R. and Blomberg, J. (1998). Comprehensive two-dimensional gas chromatography (GC × GC) as a diagnostic tool. *J. High Resolut. Chromatogr.* **21**, 63–64.

Cantley, L.C. (2002). The phosphoinositide 3-kinase pathway. *Science*. **296**, 1655–1657.

Dallüge, J., van Stee, L.L.P., Xu, X. *et al.* (2002). Unraveling the composition of very complex samples by comprehensive gas chromatography coupled to time-of-flight mass spectrometry, Cigarette smoke. *J. Chromatogr. A*. **974**, 169–184.

Dallüge, J., Vreuls, R.J.J., Beens, J. and Brinkman, U.A.T. (2002). Optimization and characterization of comprehensive two-dimensional gas chromatography with time-of-flight mass spectrometric detection (GC × GC-TOFMS). *J. Sep. Sci.* **25**, 201–214.

van Deursen, M.M., Beens, J., Janssen, H.-G., Leclercq, P.A. and Cramers, C.A. (2000). Evaluation of time of flight mass spectrometric detection for fast gas chromatography. *J. Chromatogr. A*. **878**, 205–213.

Fiehn, O. (2002). Metabolomics – the link between genotype and phenotype. *Plant Mol. Biol.*. **48**, 155–171.

Fiehn, O. (2003). Metabolic networks of Cucurbita maxima phloem. *Phytochemistry*. **62**, 875–886.

Fiehn, O., Kopka, J., Dörmann, P., Altmann, T., Trethewey, R.N. and Willmitzer, L. (2000). Metabolite profiling for plant functional genomics. *Nat. Biotechnol.*. **18**, 1157–1161.

Fiehn, O., Kopka, J., Trethewey, R.N. and Willmitzer, L. (2000). Identification of uncommon plant metabolites based on calculation of elemental compositions using gas chromatography and quadrupole mass spectrometry. *Anal. Chem.*. **72**, 3573–3580.

Hirai, M.Y., Yano, M., Goodenowe, D.B. (2004). Integration of transcriptomics and metabolomics for understanding of global responses to nutritional stresses in Arabidopsis thaliana. *Proc. Natl. Acad. Sci. USA*. **101**, 10205–10210.

Keun, H.C., Beckonert, O., Griffin, J.L. (2002). Cryogenic probe ^{13}C NMR spectroscopy of urine for metabonomic studies. *Anal. Chem.*. **74**, 4588–4593.

Kristenson, E.M., Kortyár, P., Danielsson, C., Kallio, M., Brandt, M. and Makela, J. (2003). Evaluation of modulators and electron-capture detectors for comprehensive two-dimensional GC of halogenated organic compounds. *J. Chromatogr. A*. **1019**, 65–77.

Lamas, O., Martínez, J.A. and Marti, A. (2004). Energy restriction restores the impaired immune response in overweight (cafeteria) rats. *J. Nutr. Biochem.*. **15**, 418–425.

Ledford, E. and Billesbach, C. (2000). Jet-cooled thermal modulator for comprehensive multidimensional gas chromatography. *J. High Resol. Chromatogr.*. **23**, 202–204.

Lee, A.L., Bartle, K.D. and Lewis, A.C. (2001). A model of peak amplitude enhancement in orthogonal two-dimensional gas chromatography. *Anal. Chem.*. **73**, 1330–1335.

Liu, Z. and Phillips, J.B. (1991). Comprehensive two-dimensional gas chromatography using an on-column thermal modulator interface. *J. Chromatogr. Sci.*. **29**, 227–231.

Marriott, P. and Kinghorn, R.M. (2000). New operational modes for multidimensional and comprehensive gas chromatography by using cryogenic modulation. *J. Chromatogr. A*. **866**, 203–212.

Marriott, P. and Shellie, R. (2002). Principles and applications of comprehensive two-dimensional gas chromatography. *Trends Anal. Chem.*. **21**, 573–583.

Marriott, P.J. (2002). Orthogonal GC–GC in Mondello, L., Lewis, A.C. and Bartle, K.D. (Eds), *Multidimensional Chromatography*. John Wiley & Sons, Chichester, England, pp. 77–108.

Nicholson, J.K., Foxall, P.J.D., Spraul, M., Farrant, R.D. Lindon, J.C. (1996). 750 MHz ^{1}H and ^{1}H–^{13}C NMR spectroscopy of human blood plasma. *Anal. Chem.*. **67**, 793–811.

Pendaries, C., Tronchère, H., Plantavid, M. and Payrastre, B. (2003). Phosphoinositide signaling disorders in human diseases. *FEBS Lett*. **546**, 25–31.

Phillips, J.B. and Beens, J. (1999). Comprehensive two-dimensional gas chromatography: a hyphenated method with strong coupling between two dimensions. *J. Chromatogr. A*. **856**, 331–347.

Phillips, J.B. and Xu, J. (1995). Comprehensive multi-dimensional gas chromatography. *J. Chromatogr. A*. **703**, 327–334.

Schmidt, A., Karas, M. and Dülcks, T. (2003). Effect of different solution flow rates on analyte ion signals in nano-ESI MS, or: when does ESI turn into nano-ESI. *J. Am. Soc. Mass Spectrom.* **14**, 492–500.

Scholz, M., Gatzek, S., Sterling, A., Fiehn, O. and Selbig, J. (in press). Metabolite fingerprinting: detecting biological features by independent component analysis. *Bioinformatics*..

Shellie, R., Mondello, L., Marriott, P. and Dugo, G. (2002). Characterisation of lavender essential oils by using gas chromatography–mass spectrometry with correlation of linear retention indices and comparison with comprehensive two-dimensional gas chromatography. *J. Chromatogr. A*. **970**, 225–234.

Shellie, R.A., Marriott, P.J. and Huie, C.W. (2003). Comprehensive two dimensional gas chromatography (GC × GC) and GC × GC-quadrupole MS analysis of Asian and American ginseng. *J. Sep. Sci.* **26**, 1185–1192.

Soga, T., Ohashi, Y., Ueno, Y., Naraoka, H., Tomita, M. Nishioka, T. (2003). Quantitative metabolome analysis using capillary electrophoresis mass spectrometry. *J. Proteome Res.* **2**, 488–94.

Steuer, R., Kurth, J., Fiehn, O. and Weckwerth, W. (2003). Observing and interpreting correlations in metabolic networks. *Bio informatics*. **19**, 1019–1026.

Tolstikov, V.V., Lommen, A., Nakanishi, K., Tanaka, N. and Fiehn, O. (2003). Monolithic silica-based capillary reversed-phase liquid chromatography/electrospray mass spectrometry for plant metabolomics. *Anal. Chem.* **75**, 6737–6740.

Vaidyanathan, S., Rowland, J.J., Kell, D.B. and Goodacre, R. (2001). Discrimination of aerobic endospore-forming bacteria via electrospray-ionization mass spectrometry of whole cell suspensions. *Anal. Chem.*. **73**, 4134–4144.

Wang, Y., Bollard, M.E., Keun, H. (2003). Spectral editing and pattern recognition methods applied to high-resolution magic-angle spinning 1H nuclear magnetic resonance spectroscopy of liver tissues. *Anal. Biochem.*. **323**, 23–26.

Weckwerth, W. (2004). Metabolomics in systems biology. *Annu. Rev. Plant Biol.*. **54**, 669–689.

Weckwerth, W., Ehlers, M.L., Wenzel, K. and Fiehn, O. (2004). Metabolic networks unravel the effects of silent plant phenotypes. *Proc. Natl. Acad. Sci. USA*. **101**, 7809–7814.

Weckwerth, W., Wenzel, K. and Fiehn, O. (2004). Process for the integrated extraction, identification and quantification of metabolites, proteins and RNA to reveal their co-regulation in biochemical networks. *Proteomics*. **4**, 78–83.

Welthagen, W., Schnelle-Kreis, J. and Zimmermann, R. (2003). Search criteria and rules for comprehensive two-dimensional gas chromatography-time-of-flight mass spectrometry analysis of airborne particulate matter. *J. Chromatogr. A*. **1019**, 233–249.

Wittmann, C., Kromer, J.O., Kiefer, P., Binz, T. and Heinzle, E. (2004). Impact of the cold shock phenomenon on quantification of intracellular metabolites in bacteria. *Anal. Biochem.*. **327**, 135–139.